IOP Publishing — Measurement Science and Technology

Meas. Sci. Technol. **23** (2012) 125001 (8pp) doi:10.1088/0957-0233/23/12/125001

Absolute measurement of gauge block without wringing using tandem low-coherence interferometry

Agustinus Winarno[1], Satoru Takahashi[1], Akiko Hirai[2], Kiyoshi Takamasu[1] and Hirokazu Matsumoto[1]

[1] Department of Precision Engineering, The University of Tokyo, Japan
[2] National Metrology Institute of Japan/National Institute of Advanced Industrial Science and Technology, Japan

E-mail: winarno@nanolab.t.u-tokyo.ac.jp

Received 2 June 2012, in final form 21 September 2012
Published 30 October 2012
Online at stacks.iop.org/MST/23/125001

Abstract
A novel method of gauge block measurement without wringing onto a glass platen is proposed. By using tandem low-coherence interferometry to perform remote measurements, wringing is rendered unnecessary. To measure its length, a gauge block for measurement without wringing is set several millimeters above a glass platen that is positioned on a triangle interferometer such that the distances between the surfaces of the block and the reflection surface of the platen can be measured from opposite directions. By using tandem low-coherence interferometry with a He–Ne laser as a reference length standard, gauge blocks with nominal lengths of 5, 10 and 75 mm have been measured remotely with an expanded uncertainty of about 86 nm.

Keywords: gauge block, non-wringing, absolute measurement, tandem low-coherence interferometry

(Some figures may appear in colour only in the online journal)

1. Introduction

Gauge blocks are widely used as a practical standard of length to calibrate length-measuring tools, such as micrometers and Vernier calipers. Low grade gauge blocks are calibrated by mechanical comparison, whereas high grade gauge blocks are calibrated using interferometry. Interferometric gauge block measurements based on several methods have been introduced [1–17]. However, wringing of the gauge blocks onto a platen is necessary in the interferometric method accepted by ISO [18], which is a complex process and requires a high level of operator skill [19, 20]. Furthermore, mechanical contact between the gauge block and platen can create several sources of error in measurements, and can cause physical damage to the surface of the gauge block, the platen or both. The contact between a body and the gauge block during a wringing process also influences the length of the block, and therefore several hours are needed for the system to reach thermal stabilization. This delay makes the measurement process inefficient.

Several methods of gauge block measurement without wringing have been introduced based on various different techniques [14–17]. However the majority of these methods use special phase-difference algorithms to uniquely determine the length of a gauge block without taking direct measurements of the absolute length. New measurement techniques must be considered that perform absolute length measurement without prior information on the nominal length of the gauge block and that simplify the measurement process in order to reduce operator skill requirements. In this paper, a novel method of absolute measurement of gauge blocks without wringing with an expanded uncertainty of 86 nm is proposed. By using this method, the length of gauge blocks can be remotely measured without any confusion due to fringe-order ambiguity.

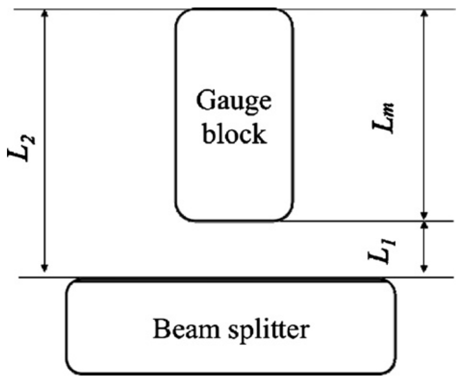

Figure 1. Basic configuration of the non-wringing method.

2. Proposed method

In this study, Michelson and triangle interferometers were connected by a single-mode optical fiber to perform remote tandem low-coherence interferometry. As a result, the length of gauge blocks could be remotely measured without the necessity of wringing the blocks onto a platen, because the signal loss due to fiber length is small.

2.1. Basic concept

To measure the mechanical length of a gauge block (L_m) without wringing it onto a platen, the gauge block is set several millimeters above a chromium-coated beam splitter. Here, L_m is defined as in figure 1, where L_1 is the mechanical distance between the top surface of the beam splitter and the bottom surface of the gauge block and L_2 is the mechanical distance between the top surface of the beam splitter and the top surface of the gauge block. Hence, $L_m = L_2 - L_1$.

From the arrangement in figure 1, to measure the length of L_2 is straightforward; however, a special technique is required to precisely measure L_1. The use of a beam splitter in this configuration gives an advantage in measuring L_1; specifically, L_1 can be measured from the bottom of the block to the upper surface of the beam splitter by low-coherence interferometry. Thus, L_1 and L_2 can be measured from opposite directions by placing the configuration in figure 1 inside a triangle interferometer.

2.2. Triangle interferometer

A schematic of the experimental setup is given in figure 2(*a*), which consists of triangle (figure 2(*c*)) and scanning (figure 2(*b*)) interferometers. The scanning interferometer is a conventional low-coherence interferometer with a super

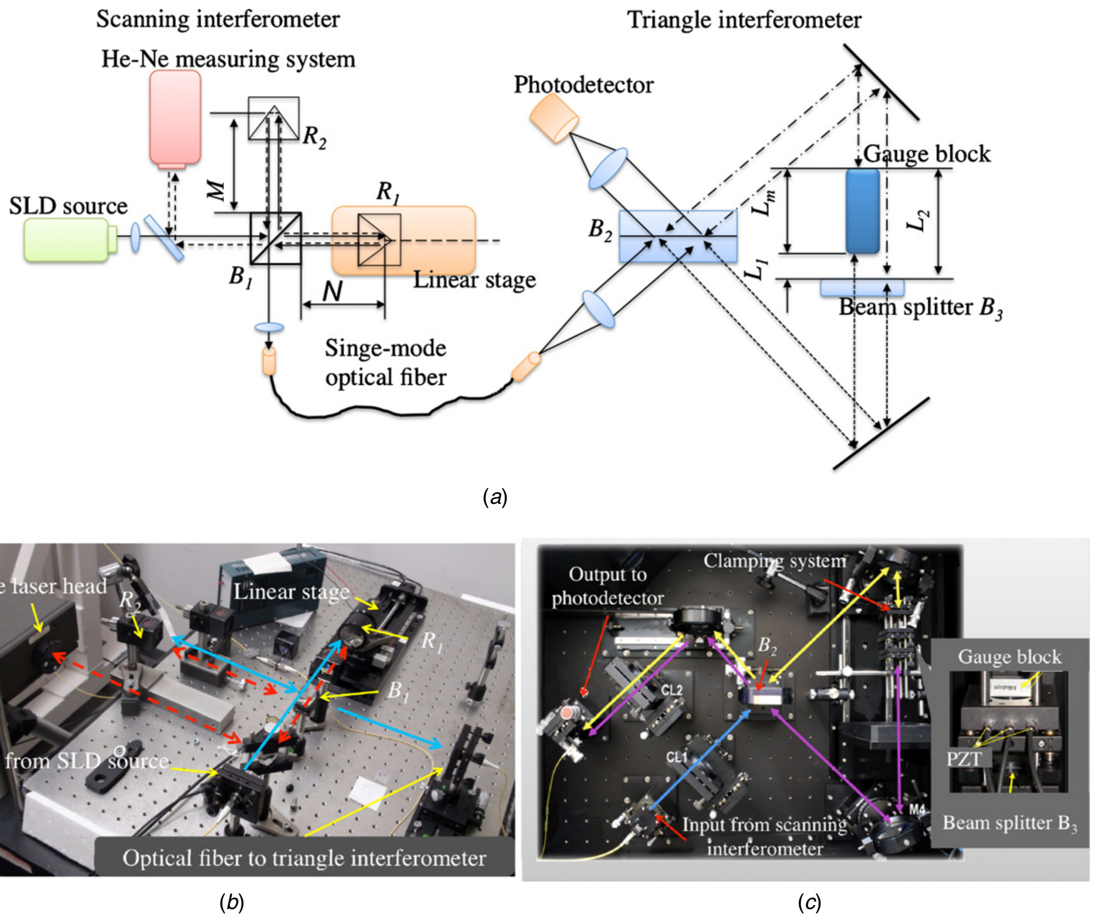

Figure 2. (*a*) Experimental setup to measure gauge blocks by tandem low-coherence interferometry. (*b*) Scanning interferometer. (*c*) Triangle interferometer.

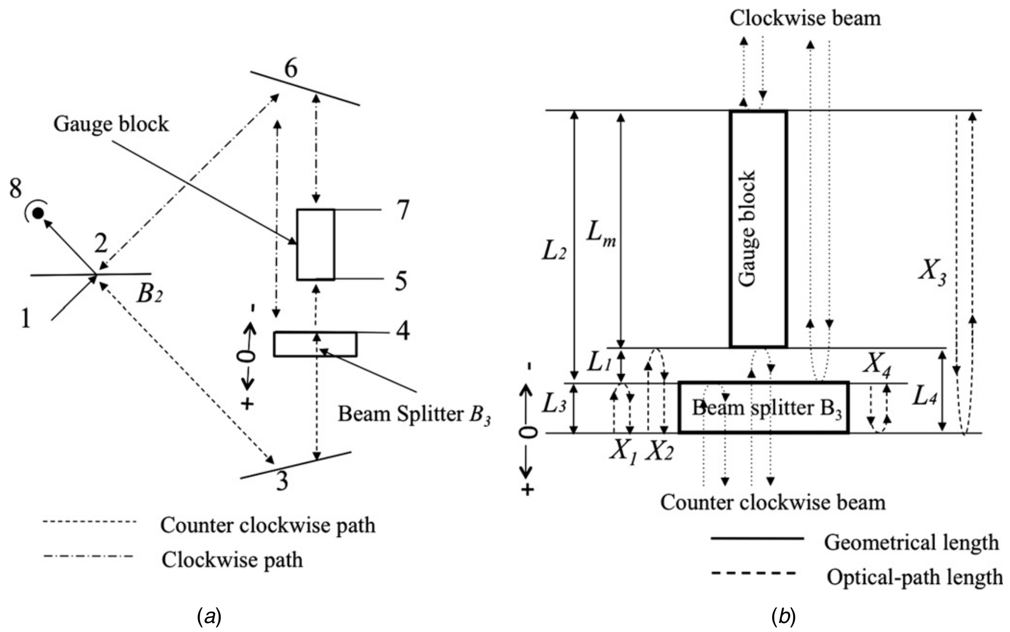

Figure 3. Detailed routes of optical paths in the triangle interferometer.

luminescent-light diode source (SLD) and it is equipped with a He–Ne laser interferometer for measuring a center-to-center distance between two low-coherence interference fringes. After passing through the single-mode optical fiber, a beam from the scanning interferometer is divided into two at the beam splitter (B_2), and these beams are then directed along clockwise and counterclockwise paths. As shown in figure 2(*a*), the beam that travels along the clockwise path is reflected when it reaches the top surfaces of the gauge and beam splitter, whereas the beam that travels along the counterclockwise path is reflected when it reaches the top surface of the beam splitter and the lower surface of the gauge.

Figure 3 shows the detailed optical paths of the triangle interferometer. The use of a glass platen with group refractive index n_g changes the length of the optical path, but it does not affect L_m.

The optical paths traveling in a clockwise direction are denoted as being positive (+), whereas counterclockwise optical paths are denoted as negative (−). Thus, L_m is calculated based on the length of optical paths, $X(i)$, and geometrical lengths, $L(i)$, from the following equations:

$$X_1 = -2(L_3 \times n_g), \tag{1}$$

$$X_2 = -2[(L_3 \times n_g) + L_1], \tag{2}$$

$$X_3 = 2[L_m + L_1 + (L_3 \times n_g)], \tag{3}$$

$$X_4 = 2(L_3 \times n_g). \tag{4}$$

Optical path differences between X_1 and X_3 (X_{31}) and between X_2 and X_4 (X_{42}) are expressed by the following equations:

$$\begin{aligned} X_{31} &= 2[L_m + L_1 + (L_3 \times n_g)] - [-2(L_3 \times n_g)], \\ &= 2L_m + 2L_1 + 4(L_3 \times n_g) \end{aligned} \tag{5}$$

$$\begin{aligned} X_{42} &= 2(L_3 \times n_g) - [-2(L_3 \times n_g) + L_1], \\ &= 4(L_3 \times n_g) + 2L_1. \end{aligned} \tag{6}$$

Hence, from (5) and (6),

$$\begin{aligned} X_{31} - X_{42} &= [2L_m + 2L_1 + 4(L_3 \times n_g)] \\ &\quad - [4(L_3 \times n_g) + 2L_1] = 2L_m. \end{aligned} \tag{7}$$

Finally, L is expressed as

$$L = \frac{X_{31} - X_{42}}{2}, \tag{8}$$

where $\frac{X_{31}}{2}$ and $\frac{X_{42}}{2}$ are equal to L_2 and L_1, respectively.

2.3. Tandem low-coherence interferometry

Since uniquely determining the length of a gauge block by a high-coherence laser, such as the He–Ne laser, requires employment of the excess fraction method [19], such light could not be easily applied in this study to measure the lengths of L_1 and L_2. Recent technological advancements, however, mean that low-coherence sources with high spatial coherence are now widely applied to length measurement. Low-coherence interferometry can achieve surface profile measurement and positioning at the nanometer scale. A tandem low-coherence interferometric method [6–11] that provides the ability to perform remote calibration was adopted in this study. The main characteristic of low-coherence tandem interferometry is that interference fringes can be observed only when the optical path differences of the triangle and scanning interferometers are equal. Therefore, the Michelson-type scanning interferometer, which functions as an optical path compensation interferometer, was set up in the present research to generate low-coherence interference fringes.

Low-coherence light emitted by a super-luminescent diode (SLD; ASLD-CWDM-3-FA; Amonics) with a center wavelength (λ) of 1544 nm is first introduced to the scanning interferometer. The beam from the scanning interferometer is then passed to the triangle interferometer through a single-mode optical fiber and is divided by the beam splitter (B_2), as

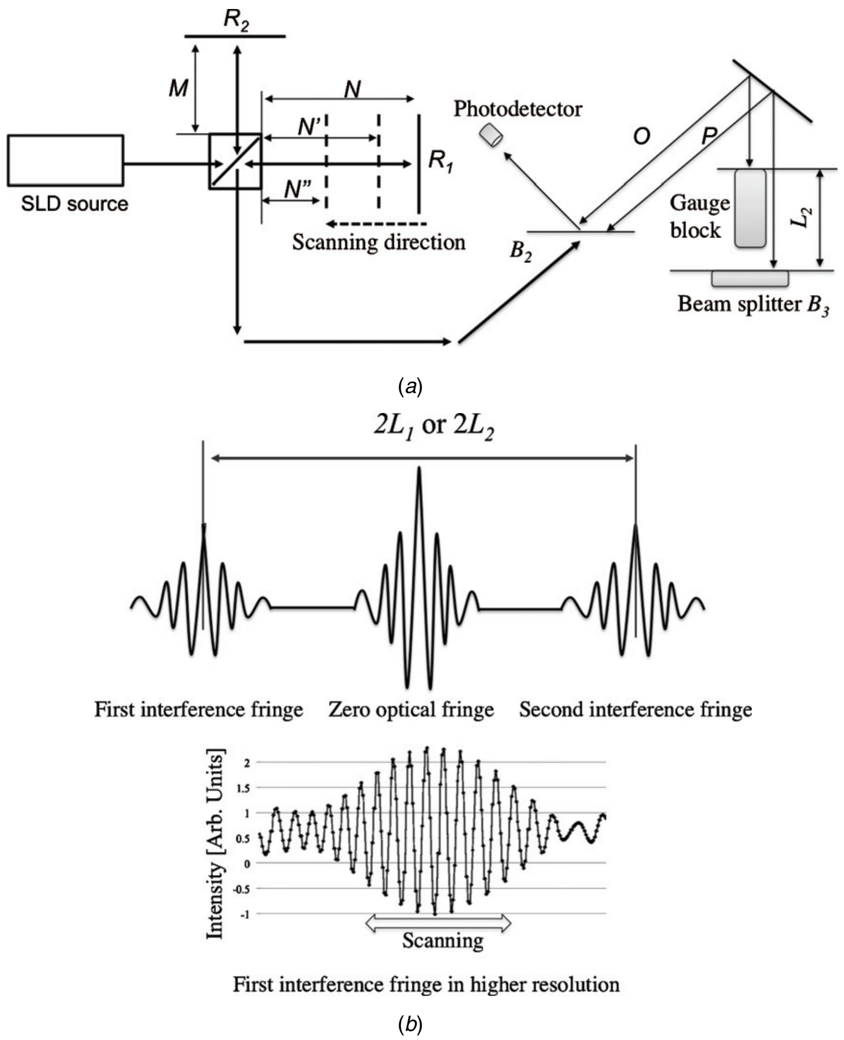

Figure 4. (*a*) An example procedure to measure L_2. The scanning retroreflector (R_1) is positioned such that $|M-N|$ and $|M-N''|$ are within 10 μm of L_2, and R_1 is then driven by PZT to perform slow scanning. (*b*) A pair of low-coherence interference fringes that correspond to $2L_1$ or $2L_2$ are generated when the lengths of optical path differences between two interferometers are equal, that is, $|M-N| = L_1$ or $|M-N| = L_2$. The first interference fringe occurs when $M < N$ and another fringe occurs when $M > N$. Therefore, half the center-to-center length between two interference fringes is equal to L_1 or L_2.

shown in figure 2(*a*). The two parts of the divided beam are thus directed to the gauge block and beam splitter by following the clockwise and counterclockwise paths. Finally, a photo-detector (2001; New Focus) collects the beams reflected from the surfaces of the beam splitter B_3 and gauge block.

3. Measurement procedure

The low-coherence interference fringes can be observed by the photo-detector when the optical path difference of the scanning interferometer is equal to the optical path difference of the triangle interferometer, that is, $|M-N| = L_1$ or $|M-N| = L_2$, where M and N are distances shown in figure 2(*a*). Interference fringes are generated by adjusting the optical path difference of the scanning interferometer to be equal to either L_1 or L_2 through adjustment of a reflector R_1 (figure 2(*a*)).

Initially, the optical path difference of the scanning interferometer ($|M-N|$) is set to be longer than the optical path difference of the triangle interferometer ($|P-O|$), $|M-N| > |P-O|$. In order to measure L_2 as shown in figure 4(*a*), initially R_1 is set so that $N - M > P - O$. The scanning retroreflector (R_1) sitting on a high precision linear stage (FC40; Sigma-tech; 70 nm positioning accuracy) is positioned such that $|M-N|$ is within 10 μm of L_2. R_1 is then driven by a piezoelectric transducer (PZT; AE02030D04F; Thorlab) to perform slow scanning in order to generate an interference fringe (figure 4(*b*)).

Using the procedure shown in figure 4(*a*), the first interference fringe occurs when the lengths of optical path differences between two interferometers are equal, that is, $N-M = L_2$. The zero optical fringe occurs when $M = N'$, and the second interference fringe occurs when $M-N'' = L_2$. Half the center-to-center length between two interference fringes is equal to L_2 when it is measured from the top direction and equal to L_1 when it is measured from the bottom direction.

The data of the low-coherence interference fringe signal and the positions of the scanning retroreflector are acquired and stored automatically by a computer. The position of the

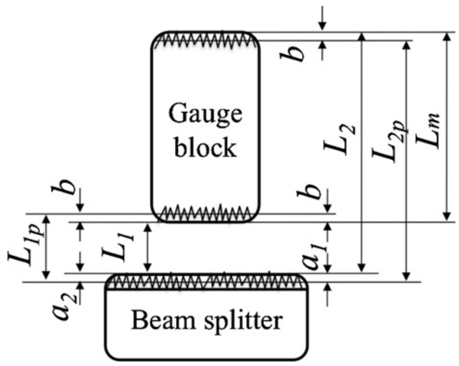

Figure 5. Derivations of phase change correction.

scanning retroreflector (R_1) that corresponds to the positions of the sampling data is precisely measured by a He–Ne length measuring system (ML100; Renishaw), simultaneously. Finally, from the position data of the scanning retroreflector, the center-to-center distances between the two low-coherence interference fringes that correspond to $2L_1$ and $2L_2$ are calculated. The center-to-center distance between two low-interference fringes is defined as the distance between two peaks of low-coherence interference fringes as shown in figure 4(*b*). The peak point of the amplitude signal is selected by analyzing the data of the interference fringe and the position of the scanning retroreflector in spreadsheet software. After the peak point is selected, the position of its point can be easily determined since every sampling datum of the inference fringe has position information, which was measured by the He–Ne length measuring system. Thereafter, the distance between two points that correspond to $2L_1$ and $2L_2$ is calculated.

The final result of the gauge measurement is expressed as a deviation length (d) from its nominal length (L) corrected by L_c:

$$d = L_m + L_c - L \tag{9}$$

$$L_m = L_2 - L_1. \tag{10}$$

L_c is evaluated from a temperature correction (l_t), a shape correction (l_G) and a refractive index correction (l_n). Hence,

$$L_c = l_t + l_G + l_n. \tag{11}$$

In the gauge block measurement using the interferometry method, 'phase correction' must be applied to the measured length because an optical length measured by the interferometry method is different from a mechanical length. It is very important to obtain the value of phase correction ($l\phi$) for a new interferometer because the phase changes take place on both ends of the gauge block. Furthermore, the phase change effect must be carefully evaluated since the use of 1544 nm wavelength in this work is different from that in conventional works [14–17, 25]. The phase change is determined by the surface roughness and properties of material. In the case of the steel gauge block wrung onto the glass platen and measured by the He–Ne laser, $l\phi$ has been reported to be about 30 nm [25]. The mechanical length of the gauge block (L_m) in figure 5 cannot be calculated directly from optical lengths L_{1p} and L_{2p} since it is necessary to calculate $l\phi$. L_{1p} is the optical distance between the top surface of the beam splitter and the bottom surface of the gauge block and L_{2p} is the optical distance between the top surface of the beam splitter and the top surface of the gauge block.

From figure 5, a correction of phase change is calculated by the following equations:

$$L_1 = L_{1p} - b - a_2, \tag{12}$$

$$L_2 = L_{2p} + b - a_1; \tag{13}$$

hence mechanical length (L_m) is

$$\begin{aligned} L_m &= L_2 - L_1, \\ &= L_{2p} - L_{1p} + 2b - a_1 + a_2. \end{aligned} \tag{14}$$

The phase correction length is expressed as

$$l_\varphi = 2b - a_1 + a_2, \tag{15}$$

where b is a phase change on steel, a_1 is a phase change from air to chromium coating and a_2 is a phase change from glass to chromium coating. The phase correction value on surface coating a_1 is different form that on a_2 because the light passes through inside the glass when L_1 is measured from the bottom direction. Theoretically, the phase change in the system is about 78 nm, which was calculated by using the equations developed by Thwaite [26] and Doi *et al* [27]. The properties of material were taken from [28] and maker specification. Our calculated value of b is 31 nm, a_1 is 29 nm and a_2 is 45 nm. The basic equation of a reflection point of the light penetration from the surface (ρ') is

$$\rho' = \frac{\lambda}{4\pi} \arctan\left(\frac{2n_0 k}{\sqrt{n_1^2 + k^2 - n_0}}\right), \tag{16}$$

where n_0 is refractivity of the source medium, n_1 is refractivity of the target medium (reflector), k is an extinction coefficient and λ is the wavelength of light [27]. Using (16), the phase correction values b (air–steel), a_1 (air–chromium) and a_2 (glass–chromium) are expressed as follows:

$$a_1 = \frac{\lambda}{4\pi} \arctan\left(\frac{2nk_{cr}}{\sqrt{n_{cr}^2 + k_{cr}^2 - n^2}}\right) \tag{17}$$

$$a_2 = \frac{\lambda}{4\pi} \arctan\left(\frac{2n_g k_{cr}}{\sqrt{n_{cr}^2 + k_{cr}^2 - n_g^2}}\right) \tag{18}$$

$$b = \frac{\lambda}{4\pi} \arctan\left(\frac{2nk_s}{\sqrt{n_s^2 + k_s^2 - n^2}}\right). \tag{19}$$

A comparison measurement was performed to get the value of the phase change of our system. A gauge block with 10 mm nominal length has been wrung onto the steel platen and put inside the triangle interferometer. Thereafter, the length of the gauge block has been measured based on the wringing method using a tandem low-coherence interferometer. Please note that the phase change effect on the wringing method has been considered to be zero. The gauge block has been measured without the wringing method as well. The lengths measured with and without the wringing method are L_W and L_{NW}, respectively. The difference of the measurement result

Table 1. E_n number of the measurement intercomparison.

	Deviation from nominal length (nm)				
Nominal length (mm)	Non-wringing method ($U = 86$ nm)	JQA Japan ($U = 40$ nm)	UME ($U = 43$ nm)	E_n [a]	E_n [b]
5	+25	−1	+3	0.27	0.23
10	+54	+73	+49	0.20	0.06
75	−120	−110	–	0.11	–

[a] E_n number between the non-wringing method and the JQA,
[b] E_n number between the non-wringing method and the UME

between wringing and without wringing is considered as a phase correction value, i.e. 85 nm, with a standard deviation of 18 nm,

$$l_\varphi = L_{NW} - L_W. \tag{20}$$

The difference between the calculated and experimental value is about 7 nm and this is probably due to some factors such as imperfect alignment and temperature instability. However, a more precise phase correction experimental setup is under development. Finally, d is expressed as

$$d = L_{2p} - L_{1p} + l_t + l_G + l_n + l_\varphi - L. \tag{21}$$

4. Experimental results and discussion

The uncertainty budget (table 2) was calculated based on the experimental data and literature study [21–24]. From (21), the combined standard uncertainty $u_c^2(d)$ is expressed as

$$u_c^2(d) = c_{L_{2p}}^2 u^2(L_{2p}) + c_{L_{1p}}^2 u^2(L_{1p}) + c_{l_t}^2 u_c^2(l_t) + c_{l_G}^2 u^2(l_G) + c_{l_n}^2 u_c^2(l_n) + c_{l_\varphi}^2 u_c^2(l_\varphi). \tag{22}$$

4.1. Sources of uncertainty

The combined uncertainty attributed to the optical length of the gauge block is evaluated from the measurement repetition of L_{2p} and L_{1p} with the sensitivity coefficient equal to 1. The standard uncertainties of $u(L_{2p})$ and $u(L_{1p})$ are 23 and 26 nm, respectively. The combined uncertainty attributed to the temperature effect $u_c(l_t)$ is evaluated from uncertainties attributed to the temperature deviation from the reference temperature measurement $u(\theta)$ and thermal expansion coefficient $u(\alpha)$. The uncertainty of nominal length $u(L)$ is zero because it is a constant,

$$l_t = \theta\alpha L. \tag{23}$$

The standard uncertainty of thermal expansion $u(\alpha)$ is estimated as about 10% from maker specification (steel gauge block, $\alpha = 10.8 \times 10^{-6}\,°\mathrm{C}^{-1}$), with a rectangular distribution. We performed measurements when the temperature difference from 20 °C (θ) was ± 0.15 °C and fluctuations were less than ± 0.3 °C over a 3 h period. Hence,

$$u(\alpha)\theta L = \frac{0.1 \times 10.8 \times 10^{-6}/°\mathrm{C}}{\sqrt{3}}(0.15\ °\mathrm{C})(L/\mathrm{mm})\ \mathrm{nm} = (0.093L/\mathrm{mm})\ \mathrm{nm}. \tag{24}$$

The temperature sensor has a reading accuracy of ± 0.05 °C, and we assume that it has a rectangular distribution. Therefore $u(\theta)$ is

$$u(\theta)\alpha L = \frac{0.05\ °\mathrm{C}}{\sqrt{3}} 10.8 \times 10^{-6}/°\mathrm{C} \times (L/\mathrm{mm})\ \mathrm{nm} = 0.3(L/\mathrm{mm})\ \mathrm{nm}. \tag{25}$$

An uncertainty related to the phase correction $u(l\phi)$ is evaluated experimentally. From (20), the combined experimental uncertainty $u_c(l\phi)$ is expressed as

$$u_c^2(l_\varphi) = c_{NW}^2 u^2(L_{NW}) + c_W^2 u^2(L_W), \tag{26}$$

where

$$c_{NW} = \frac{\partial l_\varphi}{\partial L_{NW}} = 1, \qquad c_W = \frac{\partial l_\varphi}{\partial L_W} = 1. \tag{27}$$

The experimental value of $u(l\phi)$ has been calculated to be 6 nm from the measurement performed nine times. For comparison, the theoretical value of $l\phi$ is obtained by incorporating (17)–(29) into (15). Hence, the combined uncertainty of phase correction is theoretically determined as

$$u_c^2(l_\varphi) = c_{n_s}^2 u^2(n_s) + c_{n_{cr}}^2 u^2(n_{cr}) + c_{n_a}^2 u^2(n_a) + c_{k_s}^2 u^2(k_s) + c_{k_{cr}}^2 u^2(k_{cr}) + c_\lambda^2 u^2(\lambda) + c_{n_g}^2 u^2(n_g). \tag{28}$$

By inserting optical parameters, the coefficients of sensitivity of (28) are

$$c_{n_s} = 1.12 \times 10^{-4}\lambda, \quad c_{n_{cr}} = 1.72 \times 10^{-3}\lambda,$$
$$c_{n_a} = 9.8 \times 10^{-4}\lambda, \quad c_{k_s} = 5.2 \times 10^{-5}\lambda,$$
$$c_{k_{cr}} = 1.3 \times 10^{-6}\lambda, \quad c_\lambda = 0.05, \quad c_{n_g} = 3.4 \times 10^{-4}\lambda.$$

The accuracy of optical properties is reported to be 10% [28]. Hence, the theoretical value of $u(l\phi)$ has been calculated to be 0.02 nm. Since the theoretical value is smaller than the experimental value, $u(l\phi)$ has been evaluated from the experimental value (equation (26)).

Although no correction value is considered for a shape variation (l_G), both imperfect flatness and parallelism still contribute to an uncertainty in the variation of the measured length. The standard uncertainty of shape variation $u(l_G)$ is estimated to be 5 nm. The combined uncertainty attributed to the refractive index correction $u_c(l_n)$ includes standard uncertainty parameters associated with Edlén equation $u(E)$, air pressure $u_c(p)$, partial pressure $u_c(f)$, air temperature $u(t)$ and wavelength $u(\lambda)$. The expanded uncertainty of the proposed method is expressed by $U = \sqrt{71.2^2 + 0.65^2 L^2}$ nm, where L is in mm.

Table 2. Uncertainty budget of the non-wringing method.

Standard uncertainty component $u(x_i)$	Source	Standard uncertainty $u(x_i)$	Relative standard uncertainty	Sensitivity coefficient (c_{xi})	Uncertainty contribution $u_i(d)/\text{nm} = \|c_{xi}\|u(x_i)/\text{nm}$
$u(l_{2p})$	Length of L_2	23 nm		1	23
$u(l_{1p})$	Length of L_1	26 nm		1	26
$u_c(l_t)$	(Temperature effect)				
$u(\theta)$	Temperature measurement	0.03 °C		$(10.8 \times 10^{-6}/°\text{C})/L$	$0.3L$ mm^{-1}
$u(\alpha)$	Thermal expansion coefficient[a]	0.62×10^{-6} °C^{-1}		$(20\,°\text{C}-t_g)L = 0.15L$ °C	$0.093L$ mm^{-1}
$u(l_G)$	(Variation shape)	5 nm		1	5
$u_c(l_\phi)$	(Phase change correction)	6 nm		1	6
$u_c(l_n)$	(Refractive index of air)				
$u(E)$	Edlén equation	1×10^{-8}		L	$0.01L$ mm^{-1}
$u_c(p)$	Air pressure	23 Pa		$2.7 \times 10^{-9}L$ Pa^{-1}	$0.062L$ mm^{-1}
$u_c(f)$	Partial pressure water vapor	6 Pa		$3.7 \times 10^{-10}L$ Pa^{-1}	$0.0022L$ mm^{-1}
$u(t)$	Air temperature	0.029 °C		$9.2 \times 10^{-7}L$ °C^{-1}	$0.027L$ mm^{-1}
$u(\lambda)$	Wavelength		0.01×10^{-6}	$5.4 \times 10^{-6}L$	Negligible

Combined standard uncertainty of the deviation length $u^2(d) = 1266 + 0.103\ (L/\text{mm})^2\ \text{nm}^2$

Expanded uncertainty for coverage factor $k = 2$, $U = \sqrt{71.2^2 + 0.65^2L^2}$ nm, L in mm.

[a] Steel gauge block, $\alpha = 10.8 \times 10^{-6}$ °C^{-1} and gauge block temperature $t_g = 20.15$ °C.

4.2. Experimental result

The proposed method was applied to measure gauge blocks with nominal lengths of 5, 10 and 75 mm. The measurement results of the proposed method were compared with those determined by the Japan Quality Assurance Organization (JQA) and the National Metrology Institute of Turkey (UME) by using contact-based interferometry (Mitutoyo gauge block interferometer and Köster interferometer, respectively). The reliability of measurements by the present method was examined by calculating the E_n number given by

$$E_n \frac{|T_1 - T_2|}{\sqrt{U_1^2 + U_2^2}}, \tag{29}$$

where T_1 is the measurement result of the proposed method with uncertainty U_1, and T_2 is the result of another method with uncertainty U_2. The proposed method is considered to be reliable if it obtains an E_n factor of less than 1. For example, for the 5 mm gauge block, the measurement result obtained by the proposed method produced an average difference of 26 nm compared with that of the JQA. Furthermore, for the 10 mm gauge block, the measurement result of the proposed method (+54 nm) produced an average difference of 5 nm compared with that of the UME (+49 nm).

The expanded uncertainty budget of the proposed measurement method was estimated to be 86 nm for the 75 mm gauge block, while the measurement uncertainties of the UME and JQA methods were 40 and 43 nm, respectively. Thus, from equation (29), the E_n numbers of the example 5 mm and 10 mm gauge block measurements given above are estimated to be 0.27 and 0.06, respectively. Measurements of the gauge blocks with nominal lengths of 5, 10 and 75 mm by the proposed method are compared with those produced by the JQA and UME in table 1. We confirm from the table that the proposed method is reliable since it obtained E_n numbers of less than 1.

The main sources of uncertainty came from measurement repeatability and temperature fluctuations. The temperature of the experimental room usually fluctuated by about ± 2.5 °C over a 4 h period during the daytime. To minimize the effect of this temperature fluctuation, experiments were mainly performed at midnight or in the early morning, when the room temperature was steady at close to 20 °C and fluctuations were less than ± 0.3 °C over a 3 h period. Furthermore, the experimental setup was also covered by a thermal-isolation material to minimize temperature fluctuation effects. By taking these actions, we could confirm that the experimental setup based on the proposed method could perform precise gauge block measurements without wringing onto the platen.

5. Conclusions

Gauge block measurements without wringing have been successfully performed. Gauge blocks with nominal lengths of 5, 10 and 75 mm were measured within an expanded uncertainty of about 86 nm. A comparison of the measurement results with those determined by the JQA and UME suggests that the proposed method could perform reliable measurements with the E_n number of less than 1. Therefore, this method will allow users to perform remote gauge block measurements without prior information on the nominal length and the need for a complex wringing process or high operator skill.

Acknowledgments

We thank the Ministry of Education, Culture, Sports, Science and Technology of Japan and Japan Quality Assurance Organization (JQA) for their support. We also thank the National Metrology Institute of Turkey (UME), especially Ramiz Hamid, Damla Sendogdu and Cihangir Erdogan, for participating in experiments and discussions. At present, AW is with the JQA.

References

[1] Matsumoto H 1980 Length measurement of gauge blocks using a 3.39 μm He–Ne laser interferometer *Japan. J. Appl. Phys.* **19** 713–8

[2] Lewis A J 1993 Absolute length measurement using multiple-wavelength phase-stepping interferometry *PhD Thesis* University of London

[3] Bitou Y, Hirai A, Yoshimori H, Hong F, Zhang Y, Onae A and Seta K 2001 Gauge block interferometer using three frequency-stabilized lasers *Proc. SPIE* **4401** 288–97

[4] Cuhada D S 2007 The Köster's interferometer for gauge block length measurements *PhD Thesis* Middle East Technical University, Ankara

[5] Ikonen E and Riski K 1993 Gauge-block interferometer based on one stabilized laser and a white-light source *Metrologia* **30** 95–104

[6] Hirai A and Matsumoto H 2003 Remote calibration of end standards using a low-coherence tandem interferometer with an optical fiber *Opt. Commun.* **215** 25–30

[7] Hirai A and Matsumoto H 2003 Low-coherence tandem interferometer for remote calibration of gauge blocks *Proc. SPIE* **5190** 54–61

[8] Matsumoto H, Sasaki K and Hirai A 2005 103-km-long remote measurements of end standards using low-coherence optical-fiber tandem interferometer in experimental room *Japan. J. Appl. Phys.* **44** 6287–8

[9] Matsumoto H, Sasaki K and Hirai A 2005 Remote calibration of length standards using 47-km-long optical fiber network *Japan. J. Appl. Phys.* **44** 970–2

[10] Matsumoto H and Sasaki K 2008 Remote measurements of practical length standards using optical fiber networks and low-coherence interferometers *Japan. J. Appl. Phys.* **47** 8590–4

[11] Matsumoto H and Hirai A 2009 Remote measurements of lengths by excess-fraction method using optical fiber networks and tandem interferometer *OFC: Conf. on Optical Fiber Commun.* pp 1–3

[12] Jin J, Kim Y, Kim Y, Kim S and Kang C 2006 Absolute length calibration of gauge blocks using optical comb of a femtosecond pulse laser *Opt. Express* **14** 5968–74

[13] Hyun S, Kim Y, Kim Y and Kim S 2010 Absolute distance measurement using the frequency comb of a femtosecond laser *CIRP Ann. Manuf. Technol.* **59** 555–8

[14] Nicolaus R A, Kang C and Boensch G 1998 Double-ended Fizeau interferometers with phase-stepping evaluation for measurement of cubes *Proc. SPIE* **3477** 109–15

[15] Ishii Y and Seino S 1998 New method for interferometric measurement of gauge blocks without wringing onto a platen *Metrologia* **35** 67–74

[16] Dobosz M and Iwasinska K O 2010 A new method of non-contact gauge block calibration using a fringe-counting technique: I. Theoretical basis *Opt. Laser Technol.* **42** 141–8

[17] Iwasinska K O and Dobosz M 2010 A new method of noncontact gauge block calibration using the fringe counting technique: II. Experimental verification *Opt. Laser Technol.* **42** 149–55

[18] ISO 1998 Geometrical product specifications (GPS)—length standard—gauge blocks ISO 3650:1998

[19] Tilford C R 1977 Analytical procedure for determining lengths from fractional fringes *Appl. Opt.* **16** 1857–60

[20] Matsumoto H and Zeng L 1996 Simple compensation method for wringing errors in the interferometric calibration of gauge blocks *Metrologia* **33** 1–4

[21] ISO 1993 *Guide to the Expression of Uncertainty in Measurement* ISO/IEC guide 98

[22] Decker J E and Pekelsky J R 1997 Uncertainty evaluation for the measurement of gauge blocks by optical interferometry *Metrologia* **34** 479–93

[23] Birch K P and Downs M J 1994 Correction to the updated Edlén equation for the refractive index of air *Metrologia* **31** 315–6

[24] Ciddor P E and Hill R J 1999 Refractive index of air: 2. Group index *Appl. Opt.* **38** 1663–7

[25] Leach R K and Hart A 2000 EUROMET Project 413: interlaboratory comparison of measurements of the phase correction in the field of gauge block interferometry *Metrologia* **37** 261–7

[26] Thwaite E G 1977 Phase correction in the interferometric measurement of end standards *Metrologia* **14** 53–62

[27] Doi T, Toyoda K and Tanimura Y 1997 Effect of phase changes on reflection and their wavelength dependence in optical profilometry *Appl. Opt.* **36** 7157–61

[28] Weaver J H 1984 Optical properties of metals *Handbook of Chemistry and Physics* 65th edn ed R C Weast (Cleveland, OH: CRC Press)